Biosensors and Bioelectronics 86 (2016) 609–615

Contents lists available at ScienceDirect

Biosensors and Bioelectronics

journal homepage: www.elsevier.com/locate/bios

Quantification of the vascular endothelial growth factor with a bioluminescence resonance energy transfer (BRET) based single molecule biosensor

T. Wimmer, B. Lorenz, K. Stieger *

Department of Ophthalmology, Justus-Liebig-University Giessen, Germany

ARTICLE INFO

Article history:
Received 15 June 2016
Received in revised form
12 July 2016
Accepted 18 July 2016
Available online 19 July 2016

Keywords:
Vascular endothelial growth factor (VEGF)
Bioluminescence resonance energy transfer (BRET)
Single chain variable fragment (scFv)
Ranibizumab

ABSTRACT

Neovascular pathologies in the eye like age-related macular degeneration (AMD), the diabetic retinopathie (DR), retinopathie of prematurity (ROP) or the retinal vein occlusion (RVO) are caused through a hypoxia induced upregulation of the vascular endothelial growth factor (VEGF). So far a correlation of intraocular VEGF concentrations to the impact of the pathologies is limited because of invasive sampling. Therefore, a minimally invasive, repeatable quantification of VEGF levels in the eye is needed to correlate the stage of VEGF induced pathologies as well as the efficacy of anti-VEGF treatment. Here we describe the development of three variants of enhanced BRET2 (eBRET2) based, single molecule biosensors by fusing a Renilla luciferase mutant with enhanced light output (RLuc8) to the N-terminus and a suitable eBRET2 acceptor fluorophore (GFP2) to the C-terminus of a VEGF binding domain, directly fused or separated with two different peptide linkers for the quantification of VEGF in vitro. The VEGF binding domain consists of a single chain variable fragment (scFv) based on ranibizumab in which the light- and the heavy- F(ab) chains were connected with a peptide linker to generate one open reading frame (orf). All three variants generate measureable eBRET2 ratios by transferring energy from the luciferase donor to the GFP2 acceptor, whereas only the directly fused and the proline variant permit VEGF quantification. The directly fused biosensor variant allows the quantification of VEGF with higher sensitivity, compared to the widely used ELISA systems and a wide dynamic quantification range in vitro. Our system demonstrates not only an additional in vitro application on VEGF quantification but also a promising step towards an applicable biosensor in an implantable device able to quantify VEGF reliably after implantation in vivo.

1. Introduction

Vascular endothelial growth factor (VEGF) as a strong endothelial-cell specific mitogen is affects physiological angiogenesis and lymphangenesis as well as pathological neovascularisation (Goel et al., 2013). VEGF is an anti-parallel, homo-dimeric, heparin-binding glycoprotein activating different intracellular signaling pathways through extracellular binding to the receptor tyrosine kinases (RTKs) VEGF-receptor1 (FLT1), VEGF-receptor2 (FLK1 or KDR) and VEGF-receptor3 (FLT4) located on the surfaces of endothelial cells promoting proliferation, migration, survival and vascular permeability (Kowanetz et al., 2006; Ferrara, 2004). Neuropilin receptors 1 and 2 (NRP1&2), initially identified as neuronal class3 semaphorin receptors in the developing nervous system, but also located on endothelial cells, primarily function as co-receptors, due to a lack of a catalytic intra-cellular domain, stabilizing VEGF-receptor binding (Geretti et al., 2008). The VEGF family consists of at least six subgroups (VEGF-A to VEGF-E) and the placental growth factor (PlGF). The VEGF-A subgroup is alternatively spliced to generate more or less soluble isoforms termed based on the number of amino acids (e.g.: VEGF-A165, 121, 189) (Ferrara, 2002). *In situ* hybridization demonstrated that the majority of human tumors express VEGF, indicating an involvement in tumor angiogenesis (Ferrara, 2004). VEGF expression is regulated by various cytokines or is oxygen dependent. Local hypoxic conditions such as in age-related macular degeneration (AMD), diabetic retinopathy (DR) or retinopathy of prematurity (ROP) cause an upregulation of VEGF expression in the eye, which leads to an uncontrolled formation of new but immature retinal or choroidal blood vessels impairing visual function due to edema and tractional retinal detachment. The state of the art treatment paradigm of these pathologies is the repeated injection of anti-VEGF drugs like bevacizumab (Avastin®), ranibizumab (Lucentis®) or aflibercept (EYLEA®), blocking the VEGF receptor binding

* Corresponding author.
E-mail address: knut.stieger@uniklinikum-giessen.de (K. Stieger).

http://dx.doi.org/10.1016/j.bios.2016.07.058
0956-5663/

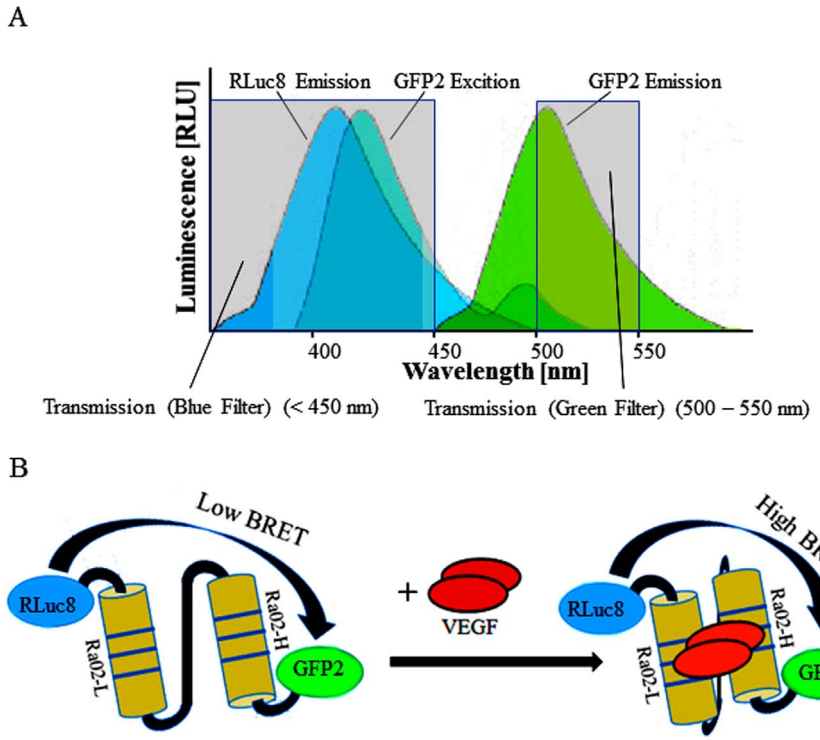

Fig. 1. eBRET2 principle. (A) RLuc8 converts coelenterazine 400a and thus generates an emission peak (~415 nm) overlapping the excitation peak of GFP2 transferring energy to the fluorophore which emits light at ~513 nm. (B) VEGF binding causes a conformational change in the biosensor by reducing the distance between RLuc8 and GFP2 and increasing the efficiency of the energy transfer which results in a higher BRET2 ratio.

domain of VEGF and thus inhibiting the VEGF induced VEGF receptor phosphorylation that leads to the activation of intracellular signaling pathways (Ferrara et al., 2004; Chen et al., 1999; Holash et al., 2002). The initial VEGF concentration before anti-VEGF treatment varies from patient to patient. Changes in visual acuity (VA) and morphologic alterations within the retina are measured with spectral domain optical coherence tomography (SD-OCT) to monitor the efficacy of the treatment occurring with delay and when VEGF inhibition is already decreasing again (Muether et al., 2012).

Biosensors offer a fast and sensitive confirmation and quantification of a wide spectrum of label-free analytes (Turner, 2013; Rea et al., 2011). Bioluminescence resonance energy transfer (BRET), a principle which uses a bioluminescent enzyme as a donor for the generation of energy that is transferred to a fluorescent acceptor molecule due to spectral overlapping, was already described by Theodore Förster in 1948 (Fig. 1A) (Foerster, 1948). This non-radiative energy transfer was extensively used to monitor and study protein-protein interactions in vitro and in living cells and tissues (Pfleger et al., 2006; De et al., 2007). Current BRET systems are mostly using the Renilla reniformis luciferase (RLuc) or related mutants with an increased light yield as the energy donor and variants of green fluorescent protein (GFP) with suitable spectral overlapping properties as the energy acceptor. RLuc´s emit light in the presence of coelenterazine derivates with different emission maxima (e.g.: $\lambda em = \sim 480$ nm for native coelenterazine (CLZ) or $\lambda em = \sim 400$ nm for coelenterazine400a (CLZ400a)) overlapping the excitation peak of GFP and thereby transferring energy to the fluorophore which emits light at a higher wavelength ($\lambda em = \sim 510$ nm). Because of the excellent spectral resolution ($\Delta\lambda em = \sim 100$ nm), the combination RLuc8 and GFP2, named after the mutational enhancement of the RLuc8´s light output and following the order of inventions (eBRET2), offers the most sensitive combination compared to other BRET systems (Loening et al., 2007). BRET systems are a useful laboratory tool not only to understand receptor function or protease activity, but also quantification of specific analytes was shown to be possible (Borroto-Escuela et al., 2013; Siddiqui et al., 2013; Wu et al., 2014; Dragulescu-Andrasi et al., 2011; Le et al., 2014).

The aim of this study was to develop protein-based, implantable biosensors for in vitro and in vivo VEGF quantification that reliably quantifies endogenous VEGF levels more sensitive than the commercially available ex vivo VEGF ELISAs (enzyme linked immunosorbent assays) (Fig. 1B). For this purpose we cloned the eBRET2 components RLuc8 and GFP2 to the N- and C-terminal part of a single chain variable fragment (scFv; Ra02) based on ranibizumab (Wimmer et al., 2015). This scFv was generated in our lab by fusing both chains together with a 6x glycine peptide linker to generate one open reading frame (orf). The directly fused biosensor molecule (RLuc8-Ra02-GFP2) was used to generate the two remaining biosensor variants RLuc8-Proline-Ra02-Proline-GFP2 and RLuc8–4xGlycine-Ra02–4xGlycine-GFP2 by PCR insertion mutagenesis (Supplementary Fig. 1).

2. Material and methods

2.1. Construction of eBRET2-VEGF-biosensors

Ranibizumab amino acid sequences (light- and antigen binding part of the heavy chain) were re-translated into DNA sequence, fused to the secretory IgG kappa leader sequence and codon optimized for the expression in mammalian cells. Both open reading frames (ORFs) were restriction cloned into pIREShrGFP (Stargene; La Jolla USA) separated with an internal ribosomal entry site (IRES). In the following step, the IRES and the heavy chain leader sequence were deleted again and a 6x glycine linker (GGC GGC GGC GGA GGA GGA) was introduced between the two ORFs, using mutagenesis polymerase chain reaction (PCR) to generate a VEGF binding single chain variable fragment (scFv) of ranibizumab

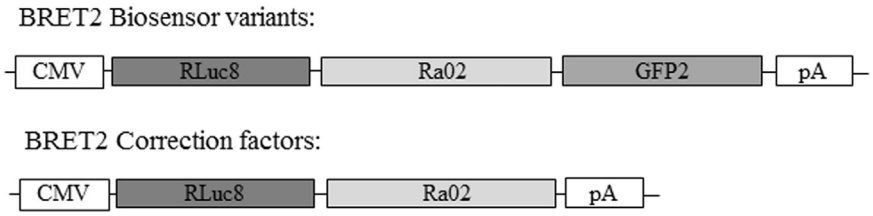

Fig. 2. Biosensor and correction factor expression constructs. (A) Biosensor variants under the control of a CMV (cytomegalovirus) promotor. Renilla luciferase (RLuc8) N-terminal fused to the ranibizumab scFv (Ra02) and GFP2 fused to the C-terminus. Directly fused or peptide-linker (L) between each biosensor domain are proline or 4x glycine. (B) Corresponding correction factors with deleted acceptor fluorophors as control for BRET2 ratio normalization.

(Ra02) (Wimmer et al., 2015). RLuc8 and GFP2 were PCR amplified and directly fused to the N- and C-terminal part of Ra02 using InFusion recombinase (Clontech; Saint-Germain-en-Laye France). Expression constructs were further introduced into pcDNA3.1 (Invitrogen, Thermo Fisher Scientific; Braunschweig) by restriction cloning and additional linkers (proline or 4x glycine) were inserted between luciferase and Ra02 as well as Ra02 and GFP2. For the generation of correction factors (cF) the GFP2 as the acceptor fluorophores were deleted again and stop codons were inserted to terminate the expression after Ra02 ORFs (Fig. 2) (Standard molecular biology techniques (Fig. S1)).

2.2. Cell culture, transfection, expression and cell lysis

HEK293 (ATCC: CRL-1573), grown in phenol-red free DMEM (Dulbeccos modified eagle media) supplemented with penicillin/streptomycin, L-glutamine (200 mM) and 10% fetal bovine sera (FBS) (all PAN Biotech; Aidenbach Germany), were transfected in 6 well plates (Greiner;) using Lipofectamine 3000 (Life Technologies; Darmstadt Germany) with 6 μg plasmids carrying the biosensor expression constructs and the corresponding correction factors. Expression was carried out for 24 h at 37 °C, 5% CO_2 in a humidified incubator. After 24 h of expression, cells were washed twice with phosphate buffered saline (PBS) and collected in luciferase lysis buffer (Promega; Mannheim Germany) using a rubber policeman. Suspended cells were transferred into a tube for two additional freeze-thaw cycles in liquid nitrogen. Lysates were cleared with centrifugation at 4 °C at 14,000 g for 5 min and transferred into fresh tubes prior to further analysis.

2.3. Western blot analysis

Equal amounts of lysates were separated with a 10% Tris-HCL SDS-PAGE (sodium-dodecylsulfate polyacrylamide gel electrophoresis) and transferred to a nitrocellulose membrane using a semidry blotting system (Biometra; Göttingen Germany). Membranes were probed with rabbit anti-RLuc (Biomol; Hamburg Germany) as 1st and goat anti-rabbit-IgG horse radish peroxidase (HRP) conjugated as 2nd antibody (Sigma Aldrich, Taufkirchen Germany). Rabbit anti-GAPDH (glyceraldehyde-3-phosphate dehydrogenase) (R&D Systems, Wiesbaden Germany) in combination with goat anti-rabbit-IgG-HRP was used as loading control.

2.4. Biosensor RLuc8 activity

10 μl of each biosensor lysate and corresponding correction factor were platted in COSTAR Lumiplates Flat White (Corning; Berlin Germany). Coelenterazine 400a (CLZ400a; NanoLight Inc.; Pinetop USA) stock (1.0 mg/ml in 100% ethanol) was diluted 1:200 in BRET2 assay buffer (PBS supplemented with 1.0 g/l D-glucose-monohydrate (Roth; Karlsruhe Germany), 0.1 g/l calciumchloride-dihydrate (Merck; Darmstadt Germany) and 0.1 g/l magnesiumchloride-heptahydrate (Merck; Darmstadt Germany)) and allowed to stabilize during 20 min. One hundred μl of the renilla luciferase substrate solution was added to the lysates and readings were taken immediately afterwards with the Tecan Infinite M1000Pro plate reader (Tecan, Groeding Austria) with open filters and an integration time of 1 s to collect photons produced by the luciferases (photons/s ≙ RLU).

2.5. Fluorescence microscopy

The fusion of the GFP2s to the biosensor variants and its activity were confirmed by fluorescence microscopy using Keyence BZ-8000 (Keyence; Neu-Isenburg Germany) with exposure times less than 1 s

2.6. Spectral scans and in vitro BRET2 assays

Spectral luminescence scans were performed from 350 to 600 nm using the Tecan Infinite M1000Pro plate reader (Tecan, Groeding Austria) with 10 μl lysate for each variant and its corresponding correction factor in luminescence scan mode in 1 nm steps with a bandwidth of 20 nm after the addition of 100 μl substrate supplemented BRET2 assay buffer.

BRET2 assay measurements were performed with equal amounts (10 μl) of biosensor variant cell lysates and the corresponding correction factor lysates. One hundred μl of CLZ400a supplemented BRET2 assay buffer were added to the variants in triplicates and measured using the dual color luminescence mode on Tecan Infinite M1000Pro plate reader (Tecan, Groeding Austria) with filters in the range of 370–450 nm (Blue filter) and 510–540 nm (Green filter). Corresponding measurements with blue and green filters were used to calculate the BRET2 ratios (BR). Normalized eBRET2 ratios were calculated using the BRET2 Eq. (1) and mean eBRET2 ratios were composed using triplicate measurements plus standard deviation (SD).

$$\text{BRET2Ratio}=\frac{\text{Biosensor(Green filter)}}{\text{Biosensor(Blue filter)}}-\frac{\text{cF(Green filter)}}{\text{cF(Blue filter)}} \quad (1)$$

2.7. BRET2 ratio kinetics, signal/background ratio and Z′ factor

20 μl of each biosensor variant and one correction factor lysate were pipetted in triplicates onto a white 96well plate for luminescence measurements, 100 μl of CLZ400a containing BRET2 assay buffer were added and luminescence was quantified in dual luminescence mode using the blue- and green filter set for BRET2. Measurement was repeated every 3 min beginning after one minute. Signal to background ratios (S/B) were calculated using Eq. (2) for each time point in triplicates plus SD. Z′ factor for screening quality assessment was calculated using Eq. (3) for each time point in triplicates plus SD.

$$\frac{S}{B}=\frac{\text{Mean Biosensor BR}}{\text{Mean correction factor BR}} \quad (2)$$

$$Z' = 1 - \frac{3*SD(Biosensor) + SD(cF)}{Mean(Biosensor) - Mean(cF)} \quad (3)$$

2.8. BRET2 ratio change in VEGF dependence

Identical amounts (20 μl) of each biosensor variant lysate were incubated with serially diluted VEGF solutions (10 μl) (10 ng/ml–100 fg/ml) at 4 °C under gentle agitation. Samples containing VEGF bound biosensors were transferred onto white luminescence 96well plates in triplicates and 100 μl of CLZ400a containing BRET2 assay buffer was added and incubated at room temperature for 45 min. The BRET2 ratio change compared to negative control (0.0 ng/ml VEGF) was measured in dual luminescence mode of the multiwell reader (Tecan, Groeding Austria).

2.9. Statistical testing

All data are reported as mean ± standard deviation (SD). All comparisons were done with students *t*-test using SigmaPlot (Systat Software Inc; Erkrath Germany) unless otherwise stated. $P < 0.05$ was considered as statistically significant.

3. Results

3.1. Biosensor construction, expression and functionality

The scFv Ra02 was used to generate three single molecule VEGF binding biosensors by fusing the RLuc8 to the N-terminal and GFP2 to the C-terminal part of Ra02 (Wimmer et al., 2015). The parental biosensor ORF was further cloned into pcDNA3.1+ and DNA linkers coding for proline and 4x glycine were inserted between the single domains by site directed PCR insertion. Corresponding correction factors were generated by deleting the fluorophore GFP2 from each biosensor variant by PCR deletion (Fig. 2). Full length biosensor expression was verified using western-blotting showing estimated molecular weights of ~100 kDA in nearly equal amounts compared with GAPDH used as loading control (Fig. 3A). RLuc8 was active in crude lysate after the addition of CLZ400a with open filter in luminescence mode. Measured luciferase light output was $106.625 \times 10^6 \pm 0.678 \times 10^6$ RLU for the direct biosensor variant, $101.146 \times 10^6 \pm 0.354 \times 10^6$ RLU for the proline variant and $60.375 \times 10^6 \pm 0.323 \times 10^6$ RLU for the 4x glycine variant compared to the negative control (11,990 ± 157 RLU) and RLuc8 ($227.665 \times 10^6 \pm 1.667 \times 10^6$ RLU) used as positive control and one example of the correction factors (directly fused) with $91.434 \times 10^6 \pm 0.271 \times 10^6$ RLU (Fig. 3B). Finally GFP2 expression in transfected HEK293 was shown for the three biosensor variants using fluorescence microscopy (Fig. 3C). These experiments prove that each component of the BRET2 VEGF binding biosensors is working as mentioned.

3.2. Bioluminescence resonance energy transfer (BRET) of biosensor variants

To demonstrate that energy is transferred from the donor to the fluorophore GFP2 as acceptor, luminescence scans were performed for each biosensor variant and corresponding correction factor after addition of CLZ400a using luminescence scan mode in 1 nm steps each with a bandwidth of 20 nm (Fig. 4A). Scans show the luciferase emission maximum peak at ~410 nm and a GFP2 emission maximum peak ~510 nm, generated through bioluminescence resonance energy transfer, for the directly fused and the proline biosensor variant, whereas the 4x glycine variant shows background noise in the region of the GFP2 peak. Correction factors just produce the predicted luciferase maximum peak at ~410 nm (Fig. 4A).

Brutto eBRET2 ratios were calculated for each biosensor variant with its corresponding correction factor. The direct biosensor

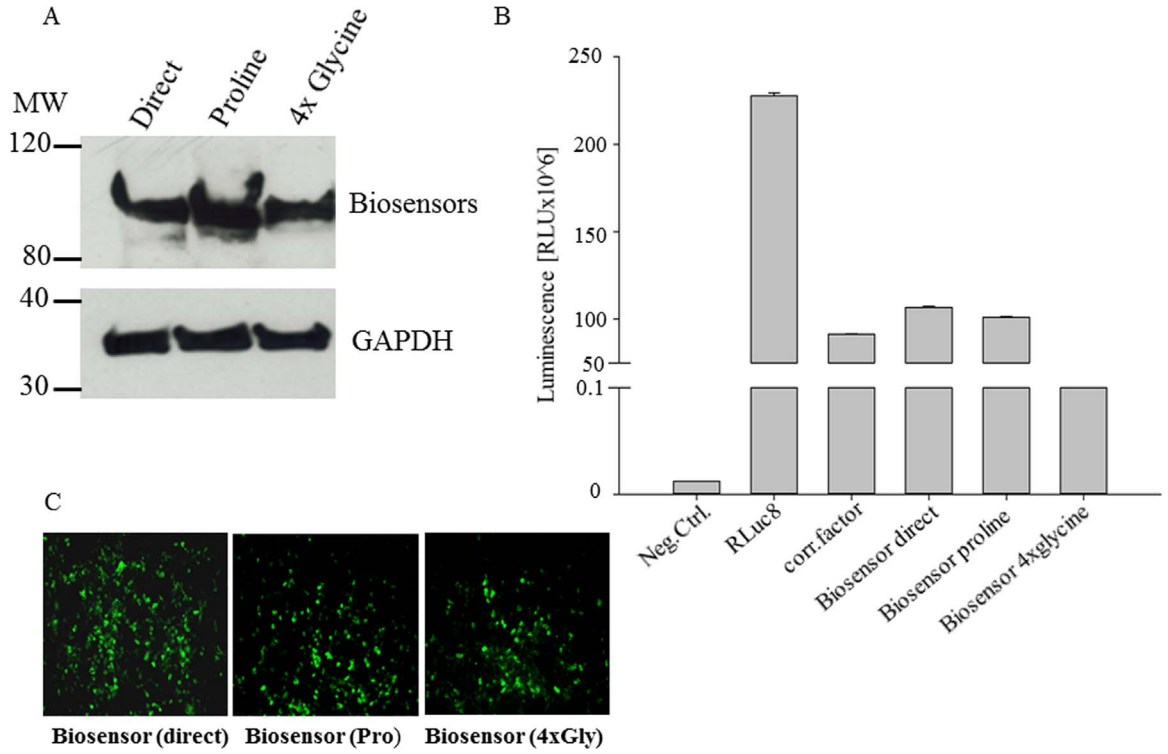

Fig. 3. (A) Western blots showing the size of fully expressed biosensor variants at near equivalent quantity. Blot is probed with a monoclonal anti-RLuc antibody and anti-GAPDH as loading control. (B) RLuc8 expression correlated to its activity. (C) Confirmation of GFP2 expressions as eBRET2 acceptors of the biosensor variants with fluorescence microscopy.

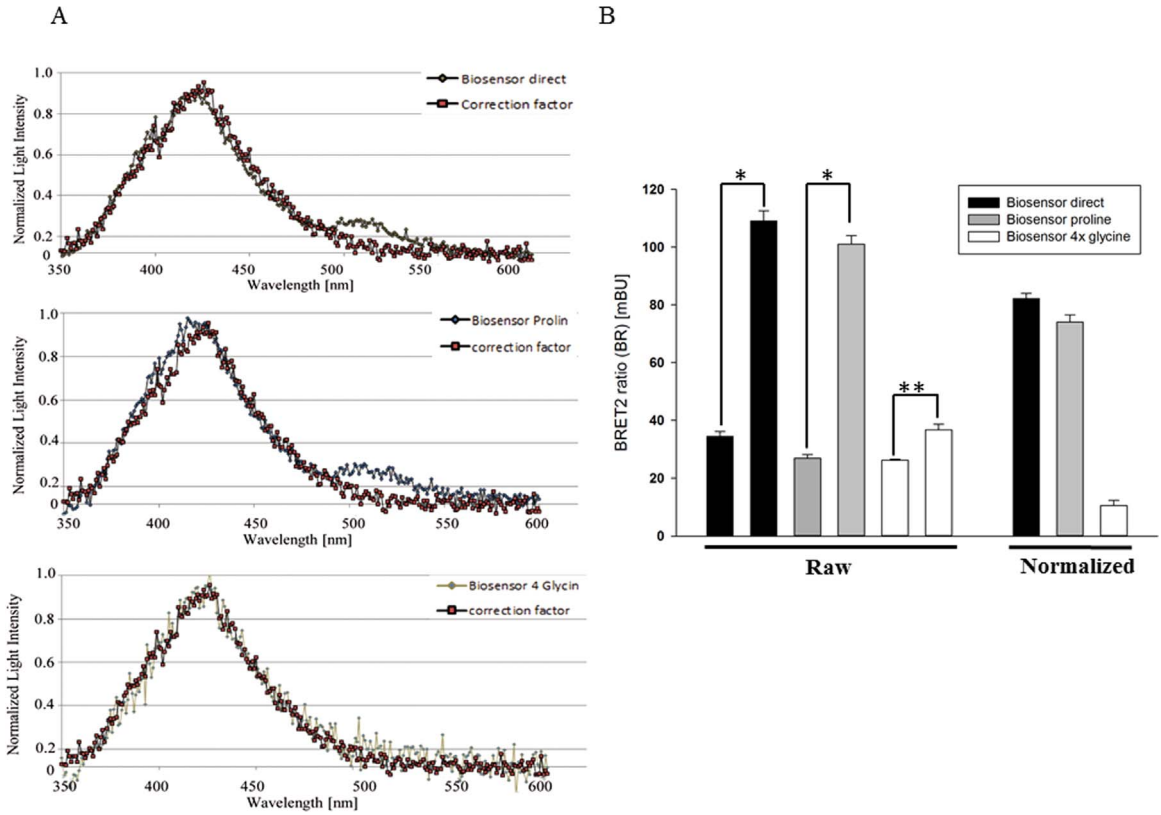

Fig. 4. (A) Spectral scans of biosensor variants with purposed correction factors in range 350–600 nm. (B) Raw and normalized eBRET2 ratios. Filter based measurements of BRET2 ratios produced from each variant and its correction factor. (*$p < 0.001$; **$p = 0.016$).

variant generates a eBRET2 ratio of 109.1 ± 3.5 mBU (milli BRET2 units) which is significantly different ($p < 0.001$) from its correction factor 26.9 ± 3.0 mBU. The proline biosensor variant generates a ratio of 101.1 ± 2.8 mBU, which is also significantly different ($p < 0.001$) to the proline correction factor of 27.0 ± 1.2 mBU. The 4x glycine variant produces a decreased but still significant ($p = 0.016$) ratio of 36.8 ± 1.8 mBU compared to its correction factor of 26.3 ± 0.4 mBU (Fig. 4B). Netto eBRET2 ratios (BR biosensor – BR correction factor) were calculated according to the BRET2 Eq. (1) with 82.2 ± 1.8 mBU for the direct biosensor, 74.1 ± 2.5 mBU for the proline variant and 10.5 ± 1.8 mBU for the 4x glycine biosensor variant (Fig. 4B).

3.3. Biosensor BRET2 ratio kinetics after substrate addition

In order to define the BR after the addition of the luciferase substrate CLZ400a was measured and calculated at different time points. The constant, maximum BR is reached after 2000 s (33 min) after substrate addition for the direct and the proline biosensor variant, whereas the 4x glycine variant did not showing any time dependence after CLZ400a addition and gives similar data as the correction factor control for this experiment, indicating that the energy is not transferred to the acceptor fluorophore for this biosensor construct (see supplements Fig. 2A).

3.4. Signal to background ratio and Z′ factor

Signal to background ratios were calculated (see supplements Fig. S2B) for each time point of the BR kinetic measurement. Values > 1 generally are different from control. BR signals of the direct and the proline biosensors produce almost constant signal to background ratios after ~1000 s, whereas again the 4x glycine variant produces S/B ratios of 1 at each time point.

Z′ factors were determined to characterize the assay performance. Z′ factors above a threshold > 0.5 generally are meant to be excellent. The direct and the proline versions have excellent Z′ factors above 0.5 for every time point calculated (see Supplements Fig. 2C), whereas the 4x glycine biosensor does not fulfil the Z′ factor criteria.

3.5. VEGF dependent change in biosensor BRET2 ratio

The increase in eBRET2 ratio (ΔBR) due to VEGF binding to the biosensor was evaluated in a serial diluted VEGF concentration range from 0.001 pg/ml to 10,000 pg/ml. Samples containing no VEGF (0.0 pg/ml) were used to normalize the change in BR. VEGF was incubated with constant amounts of each biosensor, after luciferase substrate addition and an incubation time for 45 min the light output for each sample in triplicates was measured in dual luminescence mode with a blue/green filter set. Biosensor concentrations were directly correlated to the Renilla luciferase activity, which is directly proportional to the biosensor concentration. The direct biosensor variant showed an increase in BR with increasing VEGF concentrations in dependence of the biosensor concentration itself (Fig. 5). The lower biosensor concentration tested (90,000 RLU) had its maximum change in eBRET2 ratio (ΔBR) of 9.330 ± 1.965 mBU at a VEGF concentration of 10 000 pg/ml, whereas the higher biosensor concentration tested (180,000 RLU) generated a maximum change in VEGF dependence of 18.6 ± 0.003 mBU at a concentration of 100 pg/ml. The proline version of the biosensor also generated a change with a maximum of 11.1 ± 0.0006 mBU at 10 000 pg/ml, but the dependent range was smaller from 100 pg/ml to the maximum. The 4x glycine variant did not generate any significant change in BR for each tested VEGF concentration (Fig. 5).

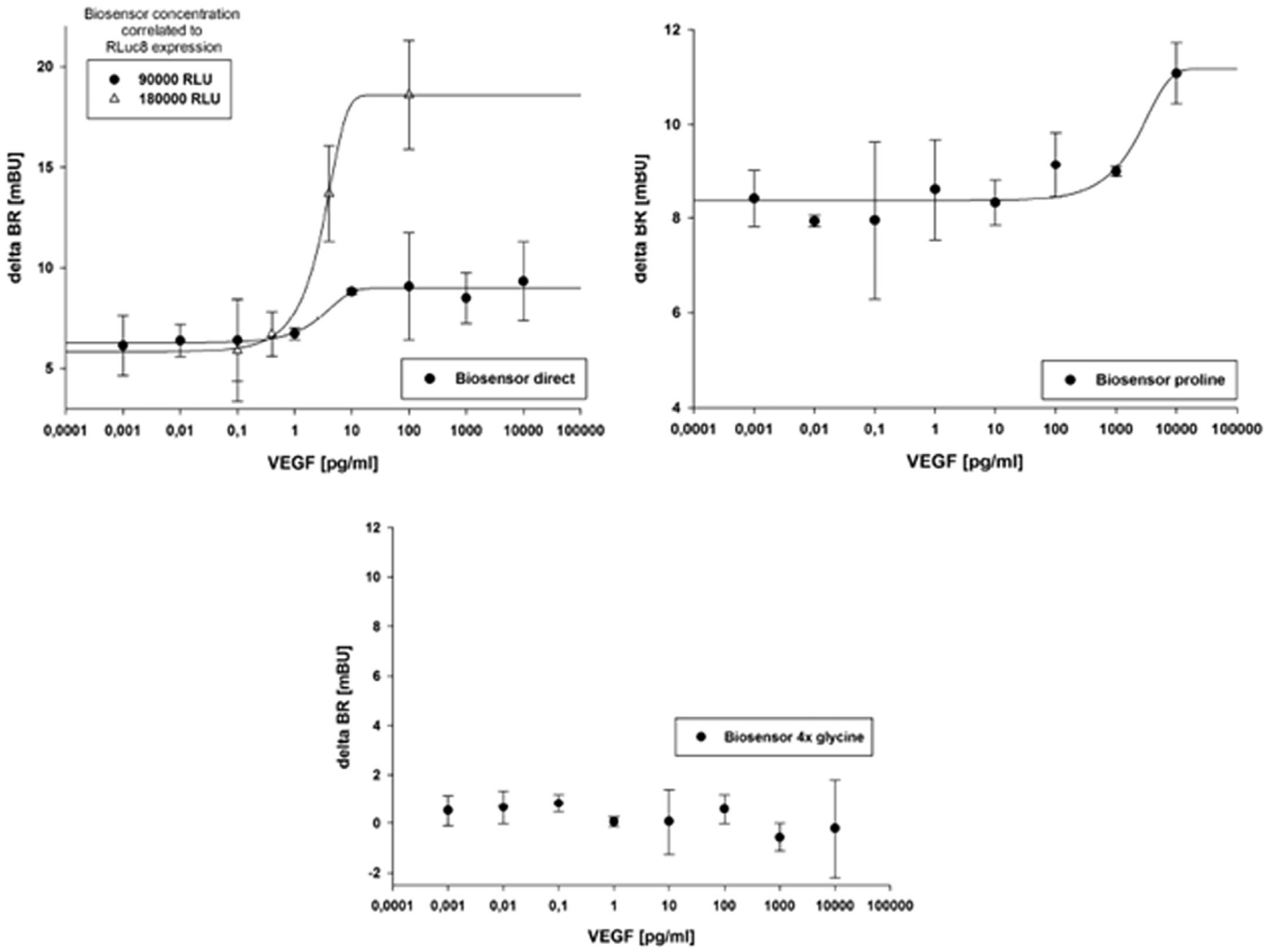

Fig. 5. Biosensor variants eBRET2 ratio change in dependence of VEGF concentration normalized to no VEGF control (0.0 ng/ml VEGF).

4. Discussion

It is still unclear how VEGF levels in the anterior chamber of the eye can be correlated to the existing levels in the inner retina where VEGF acts primarily on the choroidal and retinal vasculature. Also, the VEGF levels before and after the state of the art therapeutic treatment with anti-VEGF drugs in the eye are not yet satisfactorily investigated in terms of dose reduction and adjustment of the treatment to patient needs.

The data presented here demonstrate that VEGF quantification with an eBRET2 based, VEGF binding biosensor is possible in vitro, and potentially can be adjusted for in vivo use in an implantable device.

BRET based biosensors have been shown to be useful for the sensitive quantification of numerous analytes in vitro and in vivo (Dragulescu-Andrasi et al., 2011; Le et al., 2014). This study shows that VEGF can be quantified with the use of a single chain variable fragment, based on ranibizumab, generated in a previous work in our lab, which is fused with BRET2 components to establish single chain biosensor molecules with different peptide linkers between each single domain for optimal separation and orientation of luminescent donor and fluorescent acceptor.

The efficacy of the energy transfer from the bioluminescent energy donor to the acceptor fluorophore of the biosensor is distance and orientation dependent. BRET occurs within a defined distance of approximately 10 nm, but depends on the BRET pair used. The 3-dimensional orientation between the luciferase and the fluorophore can influence the energy transfer as well (Dacres et al., 2012; Clegg). The direct and the proline variant of our biosensor generate a measureable BRET2 signal significantly different from the controls indicating an energy transfer from the donor to the acceptor. The 4x glycine variant also produces significant BRET2 ratios in the same experiment, but with the quality control of assay parameters like the signal to background ratio and the Z ´factor, this biosensor variant shows clearly limitations in terms of analyte quantification. This may be caused by the poor orientation properties of the donor to the acceptor.

The specificity of all three biosensor variants to human VEGF is ensured with the use of the ranibizumab based VEGF binding domain as a single chain variable fragment (Ra02), which was cloned and characterized in a previous work in our lab (Wimmer et al., 2015). Ranibizumab, the original humanized F(ab) fragment derived from a murine anti-VEGF antibody, subjected to an affinity maturation process to human VEGF is well investigated and has no known unspecific binding to other growth factors (Ferrara et al., 2006).

The increase in eBRET2 ratio due to VEGF binding to the biosensor molecules is supposed to be caused by the conformational rearrangement is occurring in several proteins like binding proteins, receptors or antibodies (Le et al., 2014; Schaarschmidt et al., 2016; Sela-Culang et al., 2012). VEGF binding to the anti-VEGF domain rearranges its conformation leading to a reduction of the

distance between the donor and the acceptor and thereby generates an increase of the eBRET2 ratio (Le et al., 2014). The VEGF concentration range able to be quantified with the biosensor variants due to the conformational rearrangement shows different results depending on the linkers between the biosensors domains.

While the directly fused variant generates superior sensitivity in terms of the low concentration detection limit and the superior linear range over three log units, the proline version is still able to quantify VEGF, but is limited in sensitivity. The 4x glycine biosensor does not produce an energy transfer and therefor, is completely unsuitable for quantification. This indicates an influence on the peptide linker appearance and composition (Le et al., 2014) suggesting an influence on the increasing distance with the insertion of additional amino-acids (2x proline or 8x glycine) into the biosensor molecules. Another explanation could be the altered 3D structure with the use of a proline, which is generating a break in the amino-acid chain or the 4x glycine, which creates a more flexible peptide linker and, thus an altered energy transfer. Nevertheless, in terms of limit of the detection (LOD) the direct biosensor version (LOD $=\sim$ 0.1 pg/ml) beats any commercial available VEGF enzyme linked immunosorbent assay (ELISA) (LOD = 7.8 pg/ml) and even the more sensitive ALPHALISA technology (LOD = 2.2 pg/ml) routinely used in labs today in terms of sensitivity and quantification range.

A big advantage of the protein based biosensor variants is the general in vivo compatibility in an immobilized delivery device, which was nicely shown in an in-line monitoring of food production for the quantification of maltose. Also, after systemic administration where the biosensor is accumulated at the place of analyte appearance in vivo for rapamycin quantification was shown in rats (Dragulescu-Andrasi et al., 2011; Le et al., 2014).

5. Conclusion

We have described single molecule enhanced BRET2 biosensors for the quantification of the vascular endothelial growth factor in vitro, in preparation for in vivo quantification immobilized in an implantable device for the assessment of the VEGF concentration in vivo in the eye. The very low detection limit of the directly fused biosensor and the quantification range over several log units offer a promising step to reliably detect even low physiologic VEGF concentrations in the eye.

Conflict of interest

None of the authors has financial interests to declare.

Acknowledgments

The authors gratefully acknowledge S. Gambhir (Stanford University, CA, USA) for providing RLc8 cDNA constructs. This work was supported by a research prize from Novartis Germany (EYEnovative research prize 2014).

Appendix A. Supplementary material

Supplementary data associated with this article can be found in the online version at http://dx.doi.org/10.1016/j.bios.2016.07.058.

References

Borroto-Escuela, D.O., Flajolet, M., Agnati, L.F., et al., 2013. Methods Cell Biol. 117, 141–164.
Chen, Y., Wiesmann, C., Fuh, G., et al., 1999. J. Mol. Biol. 293, 865–881.
Clegg, R.M., ISBN 0-08-054958-6, pp. 1–58.
Dacres, H., Michie, M., Wang, J., et al., 2012. Biochem. Biophys. Res. Commun. 425, 625–629.
De, A., Loening, A.M., Gambhir, S.S., 2007. Cancer Res. 67, 7175–7183.
Dragulescu-Andrasi, A., Chan, C.T., De, A., et al., 2011. PNAS 108, 12060–12065.
Ferrara, N., 2002. Nat. Rev. Cancer 2, 795–803.
Ferrara, N., 2004a. Endocr. Rev. 25, 581–611.
Ferrara, N., Hillan, K.J., Gerber, H.P., et al., 2004b. Nat. Rev. Drug. Discov. 3, 391–400.
Ferrara, N., Damico, L., Shams, N., et al., 2006. Retina 26, 859–870.
Foerster, T., 1948. Ann. der Phys. 6, 55–75.
Geretti, E., Shimizu, A., Klagsbrun, M., 2008. Angiogenesis 11, 31–39.
Goel, H.L., Mercurio, A.M., 2013. Nat. Rev. Cancer 13, 871–882.
Holash, J., Davis, S., Papadopoulos, N., et al., 2002. Proc. Natl. Acad. Sci. 99, 11393–11398.
Kowanetz, M., Ferrara, N., 2006. Clin. Cancer Res. 12, 5018–5022.
Le, N.C.H., Gel, M., Zhu, Y., et al., 2014. Biosens. Bioelectron. 62, 177–181.
Loening, A.M., Wu, A.M., Ganbhir, S.S., 2007. Nat. Methods 4, 641–643.
Muether, P.S., Hermann, M.M., Viebahn, U., et al., 2012. Ophthalmology 119 (10), 2082–2086.
Pfleger, K.D., Seeber, R.M., Eidne, K.A., et al., 2006. Nat. Protoc. 1, 337–345.
Rea, I., Orabona, E., Lambreti, A., et al., 2011. Biomicrofluidics 5, 034120.
Schaarschmidt, J., Nagel, M.B.N., Huth, S., et al., 2016. J. Biochem. Chem. (Epub ahead of print)
Sela-Culang, I., Alon, S., Ofran, Y., 2012. J. Immunol. 189, 4890–4899.
Siddiqui, S., Cong, W.N., Daimon, C.M., et al., 2013. Front. Endocrinol. 4, 1–11.
Turner, A.P.F., 2013. Chem. Soc. Rev. 42, 3184–3196.
Wimmer, T., Lorenz, B., Stieger, K., 2015. J. Ocul. Pharm. Ther. 31, 269–276.
Wu, N., Dacres, H., Anderson, A., et al., 2014. PLOS One 9, 1–8.